

Reliability Life-Testing and Failure-Analysis of GaAs Monolithic Ku-Band Driver Amplifiers

Jeffrey A. Mittereder, *Member IEEE*
Naval Research Laboratory, Washington DC

Jason A. Roussos, *Member IEEE*
Naval Research Laboratory, Washington DC

Keith A. Christianson
Naval Research Laboratory, Washington DC

Wallace T. Anderson, *Member IEEE*
Naval Research Laboratory, Washington DC

Key Words — Arrhenius plot, Gold-tin, Field-effect transistor, Gallium arsenide, Infrared, Ku-band driver amplifier, Lognormal distribution, Monolithic microwave integrated circuit, Radio frequency, Silicon nitride, Baseplate temperature, Channel temperature.

Summary & Conclusions — Gallium-arsenide monolithic microwave integrated-circuit (MMIC) Ku-band driver amplifiers were life tested under accelerated high temperature, DC, and RF, conditions until failure. These MMIC are used in various applications such as radar and satellite communication systems. The failure mechanisms controlling their reliability must be understood in order to improve the lifetime for these and other applications. This paper discusses the experimental procedures, statistical evaluation of the data, and failure analysis of the devices. To our knowledge this is the first report of RF life testing of dual-gate driver amplifiers.

The majority of the devices failed catastrophically due to high drain current, while others failed parametrically due to low output power. Failure analysis indicates that degradation of the Si_3N_4 dielectric layer to be the main failure mechanism in these MMIC. Statistical analysis revealed an activation energy of 0.87 eV and a median lifetime of $5.8 \cdot 10^4$ hours at 140°C channel temperature, which is consistent with surface-phenomena failure mechanisms.

Mil-Spec	US Military specification
MIM	metal-insulator-metal
MMIC	monolithic microwave integrated circuit
NRL	US Naval Research Laboratory
Q#	transistor number
RF	radio frequency
S	source

Notation

I_D	D current
P_o	power output
Si_3N_4	silicon nitride
T_B	baseplate temperature
T_{ch}	channel temperature
t_{50}	median time to failure
V_D	D voltage
V_G	gate voltage

GaAs monolithic Ku-band driver amplifiers were delivered to NRL for the purpose of conducting reliability testing. Similar power amplifiers were successfully tested here in the past and the results have been presented [1 – 5].

1. INTRODUCTION

Acronyms¹

D	drain
DC	direct current
dB	10·log(power ratio)
dBm	dB relative to 1 mW
E_A	activation energy
FET	field-effect transistor
IR	infrared
I-V	current-voltage
MESFET	metal semiconductor FET

¹The singular & plural of an acronym are always spelled the same.

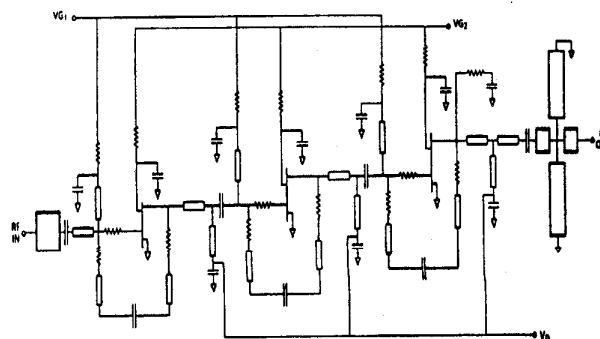


Figure 1: Schematic of GaAs MMIC Ku-band Driver Amplifier

The MMIC studied is a 3-stage variable-gain amplifier using dual-gate FET technology. Figure 1 is a schematic of the circuit; figure 2 is its design layout. The device contains:

- a 450 μm dual-gate FET in each of stages 1 & 2,
 - a 600 micron dual gate FET in stage 3,
 - associated matching and DC biasing circuitry,
- all integrated on a semi-insulating GaAs substrate. The DC biasing circuitry includes MIM capacitors. The dielectric in the MIM capacitors is Si_3N_4 film with a thickness of ≈ 100 nm. The capacitor area is $\approx 2.25 \cdot 10^4 \mu\text{m}^2$, and the capacitance is ≈ 15 pF.

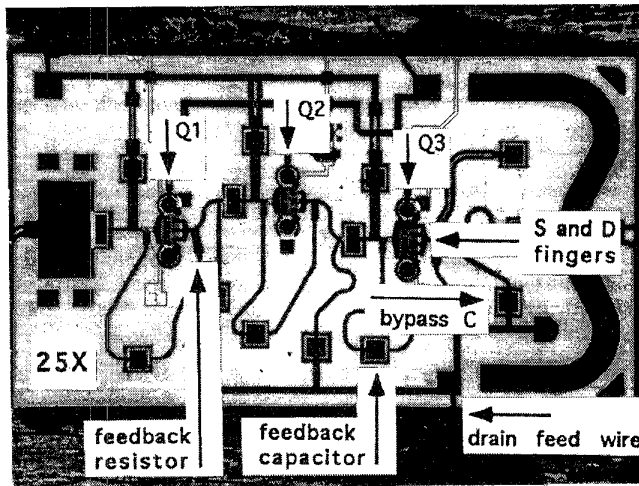


Figure 2: Structure Schematic of the GaAs MMIC Ku-band Driver Amplifier

This shows the features and the location of Q1, Q2, Q3 and the Q3 bypass capacitor.

Each chip was mounted on a gold-plated molybdenum carrier-plate with eutectic AuSn die attach. RF connection to the circuits was made through 50 Ω microstrip transmission lines. Chip capacitors were also attached to the carrier plates next to the MMIC chip, and connected in shunt with the DC bias lines for additional RF bypassing. The carrier plates were then inserted into microwave test fixtures, with microstrip-to-coaxial transitions, for reliability testing. The recommended V_D was 5.0 V, and the gate voltage was adjusted to give 120 mA of drain current. During life testing, gate #2 was grounded for each stage and a 100 μH inductor was connected in series with the drain line to eliminate oscillations. This, combined with the shunt bypass chip capacitors, formed low-pass filters. Power input was -3.0 dBm at a frequency of 15 GHz.

2. EXPERIMENTAL PROCEDURE

The amplifiers were RF life tested with a computer-controlled system under accelerated high temperature conditions at:

$$T_B = 150^\circ\text{C}, 170^\circ\text{C}, 200^\circ\text{C}.$$

Figure 3 is a schematic of the computer-controlled life test

system. The I_D & P_o are monitored 24 hours a day, and automatic shutdown is enabled if set limits are exceeded. Relevant data were logged periodically onto a disk.

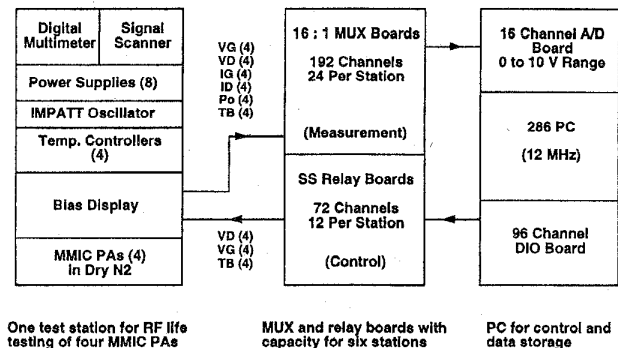


Figure 3: Schematic of the Computer-Controlled Life Test System

One RF life-test station, with provisions for 4 packaged microwave devices, was used in this study. The life-test station was designed so that the microwave input power, DC bias level, and base-plate temperature of each device could be individually monitored and controlled. Figure 4 is a schematic of a single channel of the test station. The input power to each device was adjusted by a variable attenuator, and monitored, via a 20 dB directional coupler, to ensure that the level remained constant throughout the test. To measure reflected power, another directional coupler was inserted in the reverse direction. Output power was measured by crystal detectors. Temperature control was achieved by means of a cartridge heater, a 2-wire thermocouple, and an individual temperature controller for each device. With this configuration, the baseplate temperature of each device was controlled to within $\pm 1^\circ\text{C}$.

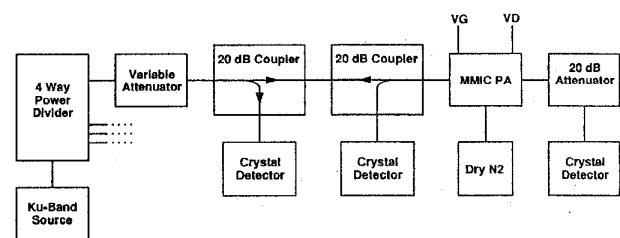


Figure 4: Schematic of a Single Channel of the Life-Test Station

The test fixtures consisted of 3 pieces. The RF launchers made direct pressure contact to the microstrip lines, which eliminated the need for wire bonding. However, wire bonding was still needed to connect the 'top plates of the chip capacitors' to the 'bonding posts on the walls of the test fixtures'. Some of the chip capacitors which were mounted on the carrier plates and wire bonded to the MMIC chips had to be replaced because they could not withstand the high temperatures used in the life tests. A nitrogen am-

bient was provided during life testing to ensure an inert atmosphere.

To ensure that all devices at a given baseplate temperature were stressed at the same channel temperature, the RF input power and DC bias levels were adjusted so that the total power dissipation was the same for each device throughout the life test. The DC power dissipation was held constant at 600 mW ($V_D = 5V$ and $I_D = 120$ mA) for all temperatures by adjusting the gate bias level, V_{G1} . Prior to life testing, the small signal S-parameters were measured, and used as prestress figures of merit. The devices were then placed on the life-test rack, and the initial values of I_D & P_o were measured at room temperature, at a baseplate temperature of 125°C (the Mil-Spec high temperature limit), and at the test temperature. These parameters were then monitored periodically throughout the life test and compared to the initial values. Devices were considered to be failed parametrically if the S_{21} gain dropped by 1 dB from its initial value anywhere across the 14 to 16 GHz band, or if the output power changed by 20% at room temperature or at 125°C.

Failure analysis was conducted on parametrically failed devices using an optical microscope with Nomarski up to 1000x. Scanning electron microscopy analysis was performed on catastrophically failed devices at 5 kV or 20 kV excitation. Infrared thermal imaging was also done prior to testing to identify possible die-attach problems and to determine hot spots on the device. Focus ion-beam cross sectioning was done on the bypass capacitors of the device with an FEI 200 FIB using a Ga beam of 70 nm.

3. RESULTS & DISCUSSION

3.1 Failure Analysis

Sixteen devices were life tested; table 1 shows a test matrix with the sample-sizes and test-conditions. The analysis did not include those samples which failed before life test or very early in the life test. Ten of the devices failed catastrophically due to high I_D , while six failed parametrically by a decrease in P_o . The majority of catastrophic failures occurred at 170°C, which was the first life-test temperature.

Five of the samples at 170°C (#H, 9, 12, 13, 15) had the drain feed wire from the chip capacitor to the GaAs MMIC (see figure 2) burned out. This bond wire was apparently acting as a fuse during a high current condition, because reconnection of this wire in all cases showed ohmic, low resistance, I-V characteristics measured drain to ground. Numerous samples (#9, 12, 13, 15, 16) showed damage to the MIM bypass capacitors associated with either Q2 or Q3. Because the shorting of this capacitor would lead to a high current condition, this element was looked at extensively. Note the similarity of this list with the burned out bonding wire list (#9, 12, 13, 15 are on both). In addition, for 4 of the 5 capacitor damaged samples (#12, 13, 15, 16) damage was seen along the microstrip bias lines,

Table 1: Test Matrix

[C \Rightarrow Catastrophic, P \Rightarrow Parametric,
TTF \Rightarrow Time to Failure (hours),
ID \Rightarrow Device identification,
Time \Rightarrow Life-test time (hours),
Tp \Rightarrow Failure type (C or P)
Fdbk \Rightarrow Feedback]

ID	Time	Tp	Failure site
5 Devices on Life-Test at 150°C			
3	2462	C	Fdbk capacitor (Q3)
8	2721	P	No obvious damage
20	5002	P	Fdbk capacitors (Q1 - Q3)
19	5219	P	No obvious damage
21	5368	C	Q2 shorted on drain side
8 Devices on Life-Test at 170°C			
H	808	C	Fdbk resistors (Q2 - Q3)
6	860	C	Fdbk resistor (Q1)
9	932	C	Bypass capacitor (Q3)
15	1124	C	Bypass capacitor (Q3)
13	1244	C	Bypass capacitor (Q3)
16	1388	C	Bypass capacitor (Q3)
12	2106	C	Bypass capacitor (Q2)
A	2500	P	Fdbk capacitor (Q3)
3 Devices on Life-Test at 200°C			
10	398	C	Q2 shorted under air bridge
9	537	C	Q1 shorted on drain side
18	585	P	S & D fingers (Q1 & Q3)

consistent with an overcurrent condition. The capacitor damage was always located near or at the airbridge of the capacitor. Figures 5 & 6 show the damage for devices #15 and #13 respectively. Possible explanations for this behavior are:

- breakdown of the Si_3N_4 dielectric layer, although it is not understood why the damage always occurs at this one location rather than appearing more randomly over the capacitor structure;
- residuals left over from the processing of the airbridge (figure 5 shows an example of the airbridge).

The resistors in the feedback portions of the circuit (see figure 2) showed damage in 3 of the samples (#H, 6, 13). For samples (#H, 6), this damage appeared to be the cause of the failure, while for sample (#13) it appeared to contribute to the failure along with the damage to the bypass capacitor of Q3. Damage to these resistors is unanticipated since in usual operation these resistors carry RF only, and thus would be not anticipated to degrade unless the RF load is far more than they were designed for. Possible explanations are:

- dielectric failure of the capacitors in series with these resistors, thus allowing excessive RF and DC currents to flow;
- damage to Q1, Q2, and/or Q3.

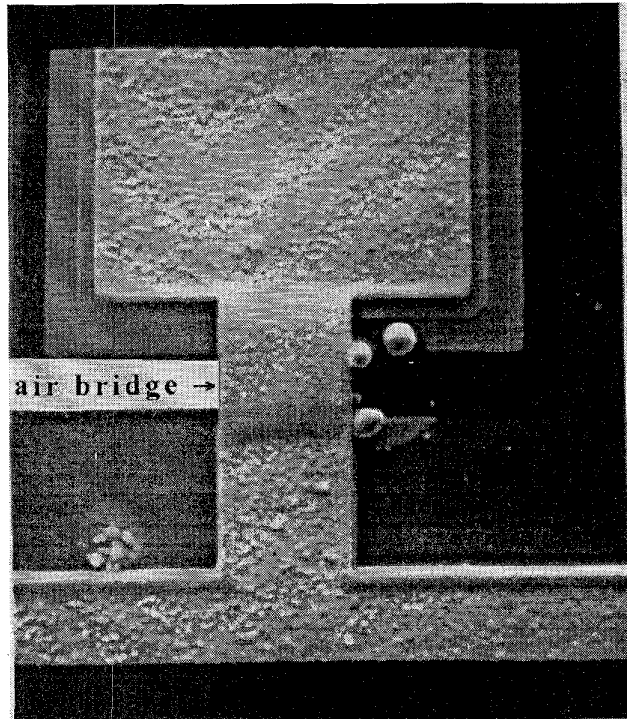


Figure 5: Example of Catastrophic Failure at Q3 Bypass Capacitor for Device #15 Life Tested at 170°C

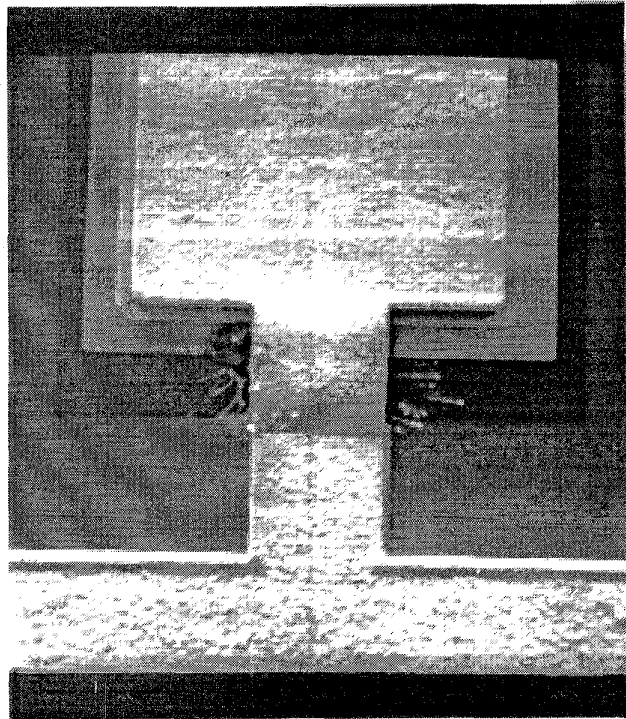


Figure 6: Example of Catastrophic Failure at Q3 Bypass Capacitor for Device #13 Life Tested at 170°C

There was no indication of damage to the visible portion of the gates or channel areas for any of the transistors of any of the capacitor-damaged samples.

Focus ion-beam cross-sectioning was performed on sample #13 at the airbridge to the Q3 bypass capacitor and in the middle of the capacitor. Figure 7 shows the underside of the airbridge which became coated with material due to the heavy ion milling. It was thought that maybe residuals had become trapped under the airbridges of the devices during processing which had subsequently caused the devices to fail. However this did not appear to be the case. Figure 8 shows a cross section from the middle of the Q3 bypass capacitor where the Si_3N_4 dielectric is sandwiched between two gold layers. The dielectric layer appears to be relatively uniform at this location, but this might not represent its condition near the airbridge.

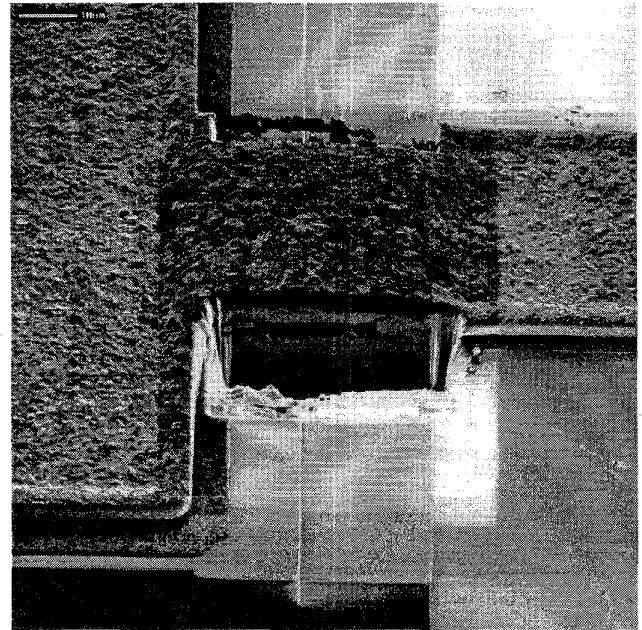


Figure 7: Focus Ion Beam Cross Section at Q3 Bypass Capacitor Airbridge of Device #13 Life-Tested at 170°C

Devices which failed parametrically showed a 20% change in output power as well as a decrease in S_{21} . Figure 9 shows output power plotted as a function of exposure time for device #A. Figure 10 shows a typical S-parameter result for device # 22 which failed parametrically at 200°C. Figure 11 presents the devices at 150°C which also showed feedback capacitor (figure 2 shows feedback capacitors) damage.

3.2 Infrared Measurements

IR measurements show a typical temperature rise of 20°C above the base plate for all 3 FET on the device. A rough idea of the variation between Q1, Q2, and Q3 was made by averaging the measured temperature for each

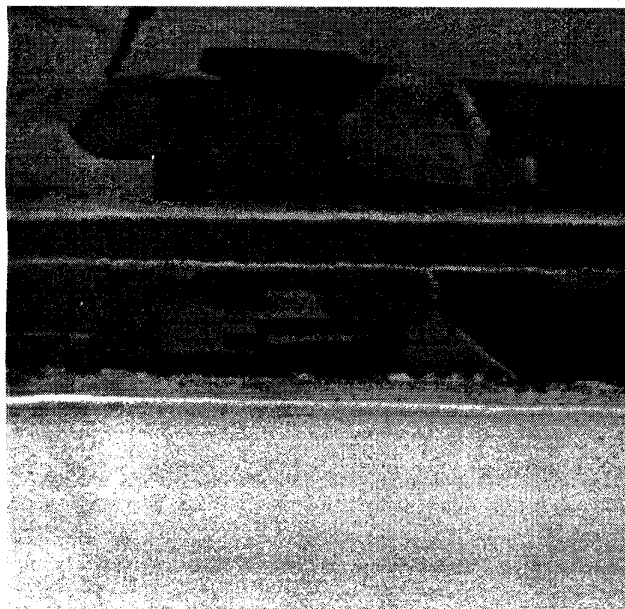


Figure 8: Focus Ion Beam Cross Section of the Middle of Q3 Bypass Capacitor of Device #13 Life-Tested at 170°C

transistor type. Such a calculation gave the average value of:

- Q1 at 119.3°C,
- Q2 at 120.4°C,
- Q3 at 118.6°C.

For samples with feature areas greater than the spatial resolution of the IR microscope, the anticipated temperature resolution is less than 0.5°C and anticipated accuracy is of the order of $\pm 1^\circ\text{C}$ (due primarily to not knowing how the thermocouple temperature is related to the baseplate

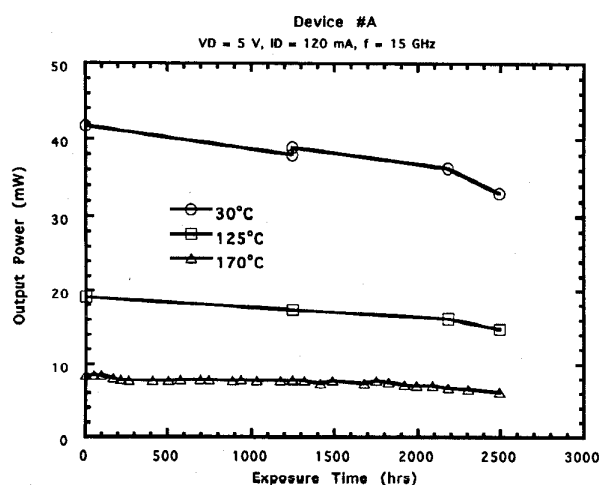


Figure 9: Output Power vs Exposure Time for Device #A RF life-tested at baseplate temperature, 170°C, and measured periodically at 30°C and 125°C. Failure by degradation in output power occurred after 2500 hours on test.

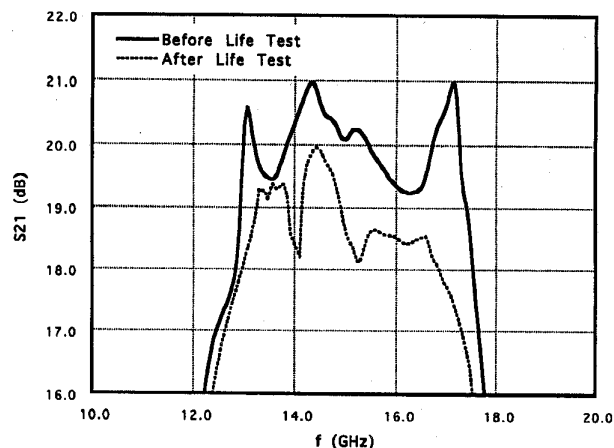


Figure 10: S_{21} vs Frequency for Device #22

Curves are before & after life testing at baseplate temperature of 200°C. Failure by degradation of S_{21} occurred after 1818 hours.

temperature). However, for the samples in this study, the features being observed are small ($< 1\mu\text{m}$) compared to the spatial resolution of the instrument ($15\mu\text{m}$), which can make the measured temperature differ from the real temperature if the temperature features have the same size as the spatial features. Also, such a small feature-size makes the emissivity corrections an average over the spatial-features emissivities, further confusing the issue. For these reasons we thus believed that all 3 transistors, as measured within the limits of the instrument, were at the same temperature under usual operation. This was confirmed by thermal modeling results from the supplier.

Temperature-measurement of the bypass capacitor of Q3 gave quite interesting results: it clearly showed the influence of heating from Q3. This capacitor is located in

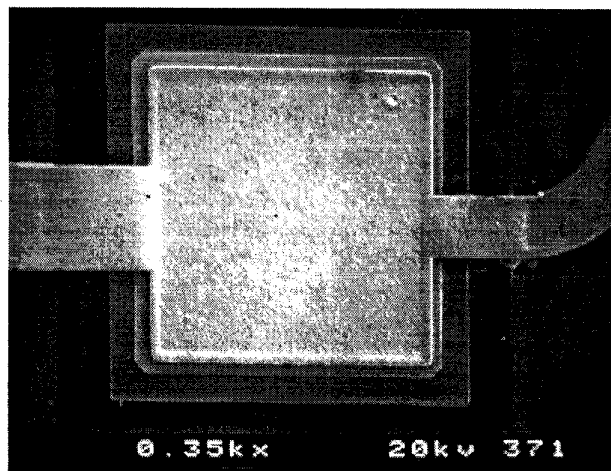


Figure 11: Example of Catastrophic Failure at Q3 Feedback Capacitor for Device #3 Life tested at 150°C.

a rough isotherm which is approximately 6°C above the baseplate, although there were major differences in temperature between the upper left corner of the capacitor and the lower right corner. For this reason a measurement location had to be defined. Since this capacitor showed failure at the airbridge, a location near this point on the GaAs was chosen for the temperature measurement spot. At this spot, the Q3 bypass capacitor exhibited an increase of 7°C .

Thermal calculation for these GaAs MESFET, based on the Cooke model [6] showed a 42°C temperature rise for each FET. The Cooke model is a precise technique for finding the FET thermal resistance. It is a simple closed-form equation derived using the assumption that the gate segments are the heat sources. The Cooke model is based on small feature sizes of the device ($< 15\mu\text{m}$) and predicts an accurate channel temperature. The infrared technique, with its limited spatial resolution of $15\mu\text{m}$, measures a temperature rise above the baseplate. The infrared scans (labeled contours) are in color and could not be included in this manuscript. The information from the Cooke model was used to determine the channel temperature for statistical analysis.

3.3 Statistical Analysis

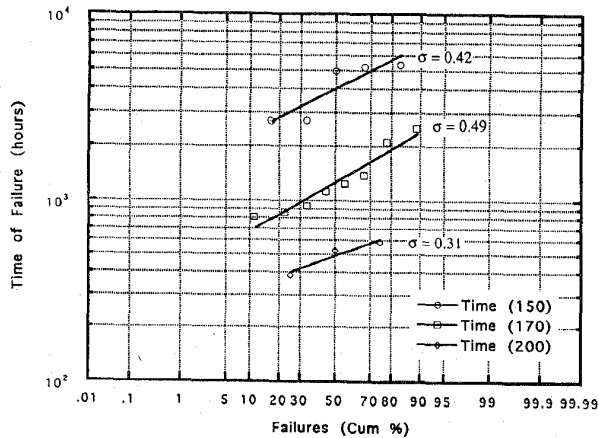


Figure 12: Lognormal Plot of Failure-Time vs Cumulative Fraction Failed

For GaAs MMIC driver amplifiers life tested at baseplate temperatures of 150°C , 170°C , 200°C .

Figure 12 shows the failure times of the life tested devices plotted vs cumulative failures, assuming a lognormal distribution. The variation in slope between the 3 temperature curve-fit lines was lowest for a Weibull distribution. However, the average correlation coefficient of the data points to the curve-fit lines is higher for the lognormal distribution. Because the lognormal distribution is typically assumed for semiconductor device reliability studies, it is used here. Usually, it would be favorable to have more

life tested devices in order to draw conclusions; however, in this case of short supply, 16 devices is considered sufficient. An Arrhenius plot of the median time to failure vs $1/T$ (T = absolute temperature) shown in figure 13 gives an E_A of 0.87 eV , and a median life of $5.8 \cdot 10^4$ hours at 140°C channel temperature. The E_A is consistent with failure mechanisms of other devices from the same supplier that were previously life tested at NRL and failed catastrophically due to degradation of the Si_3N_4 dielectric layer of the capacitors and passivation layer.

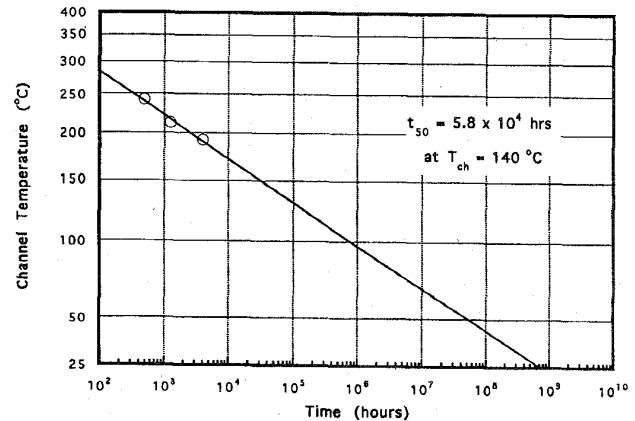


Figure 13: Arrhenius plot of t_{50} vs Channel Temperature
For the GaAs MMIC driver amplifiers RF life tested at $T_{ch} = 192^{\circ}\text{C}$, 212°C , 242°C . The dielectric breakdown failure mechanism corresponds to an E_A of 0.87 eV .

A literature search did not reveal any similar studies, but many articles produced data on the E_A of device failures and suggested failure mechanisms. Several trends regarding the relationship of the two became apparent after a table of the references was analyzed. Failure mechanisms which involved strictly temperature-related diffusion had E_A which were always within $1.3 - 2.3\text{ eV}$, and often very close to 1.8 eV [7 - 13]. A subset of temperature-related diffusion processes, such as gate metal sinking, had a similar range, and suggested a typical value of 1.6 eV [14]. In contrast, diffusion aided by electron fields (at least in HBT ?spell out?) resulted in lower E_A from $0.6 - 0.7\text{ eV}$ [14, 15]. This suggests that failure mechanisms less dependent on heat energy have lower E_A , which would apply to the devices life-tested here.

ACKNOWLEDGMENT

This work was supported by the US Office of Naval Research. We gratefully thank Maurice Daniel of DCS, Corp. for his assistance in the failure analysis.

REFERENCES

- [1] K.A. Christianson, *et al*, "Accelerated life testing and failure analysis of single stage MMIC amplifiers", *IEEE Trans. Electron Devices*, vol 41, 1994 Aug, pp 1435 – 1443.
- [2] K.A. Christianson, *et al*, "Failure analysis of MMIC power amplifiers", *Proc. 4th European Symp. Reliability of Electron Devices, Failure Physics and Analysis (ESREF 93)*, 1992; University of Bordeaux.
- [3] W.T. Anderson, *et al*, "GaAs MMIC reliability studies", *Quality and Reliability Eng'g Int'l*, vol 8, 1992, pp 295 – 300.
- [4] K.A. Christianson, *et al*, "Reliability study of a GaAs MMIC amplifier", *Proc. Int'l Reliability Physics Symp*, 1992, pp 327 – 331.
- [5] W.T. Anderson, *et al*, "GaAs MMIC reliability studies", *Proc. 2nd European Symp. Reliability of Electron Devices, Failure Physics and Analysis (ESREF 91)*, 1991, pp 411 – 422; University of Bordeaux.
- [6] H.F. Cooke, "Precise technique finds FET thermal resistance", *Microwaves & RF*, 1986 Aug, pp 85 – 87.
- [7] R. Esfandari, "Accelerated aging and long-term reliability study of ion-implanted GaAs MMIC IF amplifier", *IEEE Trans. Electron Devices*, vol 37, 1990 Apr, pp 1174 – 1177.
- [8] P. Dreike, "Analysis of parametric drift of a MESFET-based GaAs MMIC due to 125°C storage", *Reliability Physics*, 1993, pp 345 – 351.
- [9] P. Ersland, "GaAs FET MMIC switch reliability", *10th Annual GaAs IC Symp. Technical Digest*, 1988, pp 57 – 60.
- [10] Y. Saito, "Reliability testing of state-of-the-art PM Hemt MMICs three-stage low-noise amplifier", *14th Annual GaAs IC Symp. Technical Digest*, 1992, pp 153 – 156.
- [11] C.H. Chen, "RF-stressed life test of pseudomorphic In-GaAs power Hemt MMIC at 44 GHz", *IEEE MTT-S Int'l Microwave Symp. Digest*, vol 2, 1995, pp 713 – 716.
- [12] W. Roesch, "Lifetesting GaAs MMICs under RF stimulus", *IEEE Trans. Microwave Theory and Techniques*, vol 40, 1992 Dec, pp 2452 – 2460.
- [13] I. De Munari, "Thermal stability of Al/Ni gate AlGaAs/-GaAs HEMT's", *Microelectronics Reliability*, vol 35, num 3, 1995, pp 631 – 635.
- [14] K.P. Roenker, "Reliability issues for III-V heterojunction bipolar transistors", *Microelectronics Reliability*, vol 35, num 4, 1995, pp 713 – 724.
- [15] M. Hafizi, "Reliability of AlInAs/GaInAs heterojunction bipolar transistors", *IEEE Trans. Electron Devices*, vol 40, 1993 Dec, pp 2178 – 2185.

AUTHORS

Jeffrey A. Mittereder; Naval Research Laboratory, Code 6855; 4555 Overlook Ave, SW; Washington, DC 20375 USA.
Internet (e-mail): mittereder@estd.nrl.navy.mil

Jeffrey A. Mittereder (born 1961, Member IEEE) received the BS (1984) in Metallurgical Engineering & Materials Science with Electronic Materials Option from Carnegie-Mellon University, the MS (1991) in Materials Engineering & Solid Mechanics from George Washington University, and is completing a PhD in Solid State Electronics at George Mason University. He is with the Reliability Science Section at the Naval Research Laboratory, and is working on reliability life testing and failure analysis of GaAs devices.

Jason A. Roussos; Naval Research Laboratory, Code 6855; 4555 Overlook Ave, SW; Washington, DC 20375 USA.
Internet (e-mail): roussos@estd.nrl.navy.mil

Jason A. Roussos (Member IEEE) received the MS (1990) in Electrical Engineering from the John Hopkins University. He is with the Reliability Science Section at the Naval Research Laboratory, where his main responsibilities are in microwave characterization and MMIC reliability.

Dr. Keith A. Christianson; Naval Research Laboratory, Code 6855; 4555 Overlook Ave, SW; Washington, DC 20375 USA.
Internet (e-mail): christianson@estd.nrl.navy.mil

Keith A. Christianson received the PhD (1985) in Materials Science & Engineering from Northwestern University. He is with the Reliability Science Section at the Naval Research Laboratory, where he is involved with microwave device reliability.

Dr. Wallace T. Anderson; Naval Research Laboratory, Code 6855; 4555 Overlook Ave, SW; Washington, DC 20375 USA.
Internet (e-mail): anderson@estd.nrl.navy.mil

Wallace T. Anderson (Member IEEE) received the BA, MA, and PhD in Physics from the University of California, Berkeley. He joined the Naval Research Laboratory in 1977 and began working on semiconductor failure mechanisms. He is Head of the Reliability Science Section.

Manuscript TR97-001 received: 1997 January 9;

revised: 1997 November 10

Responsible editor: P. Lall

Publisher Item Identifier S 0018-9529(98)06967-X